Research Square

Preprints are preliminary reports that have not undergone peer review.
They should not be considered conclusive, used to inform clinical practice,
or referenced by the media as validated information.

Flocks in Flux: Emergent Dynamics of a Fragmenting Migratory Roost Network

William DeMott

will.demott@gmail.com

University of Oklahoma https://orcid.org/0000-0003-1175-808X

Maria Belotti
Wenlong Zhao
Subhransu Maji
Gustavo Pérez
Daniel Sheldon
Jeffrey Kelly

Article

Keywords: Tree Swallows, migratory networks, aerial insectivores, aeroecology, community ecology, stopover, network analysis, animal aggregation, complex systems

Posted Date: September 22nd, 2026

DOI: https://doi.org/10.21203/rs.3.rs-10844186/v1

License: This work is licensed under a Creative Commons Attribution 4.0 International License.
Read Full License

Additional Declarations: There is **NO** Competing Interest.

Title: Flocks in Flux: Emergent Dynamics of a Fragmenting Migratory Roost Network

Authors: Will DeMott[1], Maria Belotti[2], Wenlong Zhao[3], Subhransu Maji[3], Gustavo Perez[3], Daniel Sheldon[3], Jeffrey Kelly[1]
[1]*School of Biological Sciences, University of Oklahoma, Norman, OK, United States*
[2]*Natural Resource Ecology and Management, Oklahoma State University, OK, United States*
[3]*Manning College of Information & Computer Sciences, University of Massachusetts Amherst, Amherst, MA, United States*
Emails:
Will DeMott – will.demott@gmail.com
Jeffrey Kelly – jkelly@ou.edu

Keywords: Tree Swallows, migratory networks, aerial insectivores, aeroecology, community ecology, stopover, network analysis, animal aggregation, complex systems

Statement of Authorship:
Will DeMott conceived the study, performed all analysis, and wrote the first draft of the manuscript. Maria Belotti assisted in quantifying bird-count estimates of roost sizes, developing methods in data filtering and organization, and providing manuscript revisions. Wenlong Zhao, Gustavo Perez, and Subhransu Maji developed the machine-learning pipeline and provided roost date/location data. Dan Sheldon oversaw machine-learning system development and contributed substantially to revisions. Jeffrey Kelly assisted in study design, data interpretation, and manuscript review.

Funding Declaration:
This material is based upon work supported by the National Science Foundation under Grant NSF-GCR-2123404.

Correspondence:
Will DeMott
Department of Biology
University of Oklahoma
730 Van Vleet Oval
Norman, OK 73019, USA
will.demott@gmail.com

Data Availability Declaration:
The data that support the findings of this study are openly available in Github at https://github.com/willdemott/flocks-in-flux.

Competing Interest Declaration:
The authors declare that they have no known competing financial interests or personal relationships that could have appeared to influence the work reported in this paper.

Abstract

Large-scale animal aggregations function as complex systems where emergent structures such as herds, schools, or roosts govern the movement of populations across entire continents. Despite the importance of these systemic behaviors, observing them at a continental scale has remained a significant challenge. The detection of aerial insectivore roosts on weather radar poses an opportunity to study an aggregation network on such a scale. With decades of radar-derived Tree Swallow (*Tachycineta bicolor*) migratory roost sizes and locations, coupled with average daily roost switching rates, we constructed a 19-year long multiplex network of roost-to-roost movements across the Atlantic Flyway and assessed how its scale, composition, and topology have responded to changes in bird abundance. Our novel method revealed nonrandomly delineated roost communities, nonlinear structural dynamics, and an overall fragmentation and contraction of the network as bird abundance has declined. These results are the first to reveal the structural dynamics of a single-species animal aggregation network on a continental scale, providing a new framework for assessing the stability of collective systems under environmental stress.

Introduction

Animal Aggregations

Animal aggregations are inspiring phenomena that occur across almost all taxa, enlightening researchers across fields (Parrish & Edelstein-Keshet 1999, Sumpter 2006). Such aggregations have been studied for decades in light of their complexity and emergent properties, from information-exchange in ant colonies, to swarm intelligence in flocks of birds and schools of fish (Hassanien & Emary 2018). These emergent properties, and the individual-level behaviors that produce them, have been used to design systems of our own, such as communication networks, transportation networks, and computational networks (Stützle et al. 2011, Tang et al. 2021). Despite this broad interest, empirical studies have been largely limited to local, isolated aggregations, and have faced significant challenges to observing their large-scale structures (Hughey et al. 2018).

Tree Swallow Roosting Behavior and Ecology

Aggregations serve many different functions, but in the case of avian roosts, the drivers have been hypothesized to vary from predator evasion, information sharing, and patch-sitting (Murray 1969, Ward & Zahavi 1973, Caccamise & Morrison 1986). Despite uncertainty surrounding the adaptive value of these gatherings, significant work has been done studying the gatherings of Tree Swallows (*Tachycineta bicolor*), a North American aerial insectivore whose roosts can host up to hundreds of thousands of individuals and occur in the same location for decades and even centuries (Bent 1942, Burney 2002).

Certain species of avian aerial insectivores (particularly Tree Swallows and Purple Martins (*Progne subis*)) will form these communal roosts during both their migration and their nonbreeding seasons (Winkler 2006). It has previously been hypothesized that their migratory roosts act as

steppingstones in a gradual, continuous migration south (Winkler 2006). However, recent movement data indicate that Tree Swallows remain at their staging regions for an average of 58 days, likely to perform their complete molts, before jumping directly to their nonbreeding grounds (Knight et al. 2018). During these extensive stays in their stopover regions, Tree Swallows will forage during the day and aggregate at roosts each night, typically in wetland reed beds (Winkler 2006). When dawn breaks, the roost emerges all at once into the airspace, and is regularly captured by weather radar as distinct ring-like shapes (Eastwood et al. 1962).

Despite the tendency for roosts to appear at the same locations for years, and even centuries, individuals are not fully faithful to one roost site (Bent 1942, Laughlin et al. 2014, Knight et al. 2018). Daily roost switching has been observed during the nonbreeding season, forming connections between locally adjacent roosts (Laughlin et al. 2014). Though the motivations behind these movements are unknown, they are thought to buffer roost-site disturbance events, and the non-random decisions underlying them are consistent with group organizational strategies that facilitate information transfer of ephemeral foraging sites (Ward & Zahavi 1973, Lewis 1995, MacGregor et al. 2020). Despite a lack of understanding behind the behavior, predictable roost-to-roost movements emerge from these individual-level decisions, and the resulting structure can be conceptualized as a network of roost-to-roost movements with emergent properties. Such properties are expected to reflect dynamic behaviors in response to changes in abundance, as observed in other complex systems (Dunne et al. 2002, Drake & Griffen 2010, Clements et al. 2019, Beck et al. 2024). Provided that Tree Swallows have experienced population declines of ~40% in the last 50 years (Hostetler et al. 2024), likely due to combined effects of habitat loss, climate change, and pesticides (Spiller & Dettmers 2019), we can expect such declines to have some effect on the network's structure.

Network Analysis

Network analysis has been a crucial tool in understanding the dynamics and functionality of complex ecological systems and biological phenomena across topics and scales (Bascompte 2007, Trøjelsgaard & Olesen 2016). Network analyses have also been applied extensively to animal roosts, particularly bats (Rhodes et al. 2006, Fortuna et al. 2009, Chaverri 2010, August et al. 2014, and Zeus et al. 2018) and birds (Evangelista et al. 2017, Watts & Dyer 2018, le Roux & Nocera 2021), with a wide variety of focus ranging from social networks to disease transfer networks and even group behavior upon roost entry. Despite the wide range of network applications performed on roost systems, there has been no application of a large-scale, multi-level network study of roost-to-roost movement networks, which may reveal temporal changes in network topology and behavior on a formerly unobserved scale.

To assess how Tree Swallow migratory roost networks change over time, we constructed a multiplex (annually layered) network of migratory Tree Swallow stopover roost sites by leveraging radar data, machine-learning, citizen science, and network science, notably creating what is the largest-studied spatial dataset of roost emergences to date. The constructed network consists of roost sites as nodes, annual movement rates between roosts as spatial edges, and roost persistence across years as temporal edges. Spatial edges between adjacent roosts were quantified as the estimated frequency of roost-to-roost movements within a year, calculated with adjacent roost sizes, distance, temporal overlap, and approximate roost-switching rates derived by Laughlin et al. (2014). Temporal edges were created to represent roost-site persistence across years, and were weighted as the average daily roost size in the latter year. Since Tree Swallows have been observed to remain in local roosting regions during migration for extensive periods (Knight et al. 2018), we expected subnetworks of frequent local roost-switching to occur. To verify the presence

of these subnetworks, and determine their strength of delineation, we used a random-walk algorithm to measure the network's modularity and assign module identities to clusters of roosts (hereafter referred to as roost "communities").

We used this constructed network to ask if **1) roost networks form community-based structures emergently and 2) reorganize nonlinearly (disproportionately or dissimilarly) in response to changes in total bird abundance.** Demonstrating supporting evidence of these hypotheses would show that migratory roost networks follow scaling laws and feedback principles which govern self-organization in complex systems. To investigate, we searched for nonrandom delineations of roost communities and distributions of bird movements within communities to validate community-based structure, and then assessed the effects of population size on network demographics and structural characteristics using both generalized additive models and linear models.

Methods

Radar Data

To collect data on roost locations and sizes with a daily resolution, we used NEXRAD weather radar data, which captures the morning emergence of roosts. Estimates of the roost sizes were calculated with radar-reflectivity, a product which measures the density of the material in the airspace. These data have been used extensively in studying roosts (Eastwood et al. 1962, Russell & Gauthreaux 1998, Kelly et al. 2012, Bridge et al. 2016, Van Den Broeke 2019, DeMott et al. 2023) and have only recently been made accessible on large spatiotemporal scales (Chilson et al. 2019, Cheng et al. 2020, Belotti et al. 2023, Deng et al. 2023, Perez et al. 2024), with this study being the largest yet. We aimed to collect all years of radar derived roost data for Tree Swallows' eastern migratory range (Supp. Fig. 1). Due to missing radar-station data in the earlier years of the

NEXRAD program, we only analyzed years in which data were continuously available from all stations (2005-2023).

Roost Detection

To identify roost locations and sizes, we used a machine learning system developed by Perez et al. (2024), which was trained on manually screened roost detections, and successfully identifies and tracks the vast majority of roosts by utilizing a high-sensitivity detection threshold (0.05) while achieving an average precision at intersection-over-union threshold 0.5 ($AP^{IoU = .50}$) of 56%. The system is a convolutional neural network that identifies roosts based on imagery (ring-shaped patterns) derived from reflectivity and correlation coefficients. The machine-learning system produces roost "tracks", a series of geographic bounding boxes that encapsulate the roost over each scan, capturing the full emergence which typically occurs within one hour (~5 scans, collected in 5–10-minute intervals).

Roost-Size Calculation

We calculated roost size estimates using base reflectivity and the radar cross section of a tree swallow, which was derived by its average weight (21.2 grams, Dunning et al. 2007). We associated surface area through weight based on the formula RCS = 0.699 × log(mass) found in Horton et al. (2019). We based our remaining bird-counting calculations on formulas developed and shared in Chilson et al. (2012), assuming an even distribution of Tree Swallows within radar sampling spaces.

For each frame of each track, bounding-boxes were transformed into bounding-circles with identical center and radii, and bird counts were summed across the lowest two elevation angles (where an average of 95.1% of track reflectivity occurred). Finally, the scan with the maximum count was used as the final estimated roost size for that day.

Data Cleaning

Our initial dataset created by the machine learning system contained roost tracks that were contaminated with weather and/or anomalous propagation, which can cause over-estimations of roost sizes. Additionally, the initial dataset contained erroneous tracks that were either false-positive detections, detections that did not accurately track roosts, and/or double-detections of roosts. To clean these data, we first removed all roost-detections outside of the Tree Swallow migratory period (July 5th – Nov 23rd, Fink et al. 2023). We then removed double-detections by identifying tracks with matching dates and within 3km of one another, removing the track with either the larger distance from the radar station (for inter-station overlaps), or the shorter track-length (for intra-station overlaps). The machine-learning system also occasionally mistakenly switched target roosts, causing frames to jump across the sampling range, and so any track-frames that were more than 40km from the prior sequential frame were removed.

To identify persistent roost sites with multiple detections and remove false positives such as weather, we used a spatial clustering algorithm to detect persistent roost emergences. Due to the variation in both the spatial range and point density of roost detections, we used a hierarchical density-based spatial clustering algorithm with a minimum cluster-size of 10 points, which adaptively detects clusters with varying densities (Ester et al. 1996, Esri 2024). By removing points outside of clusters, we effectively removed the majority of ephemeral roosts and false-positive detections. We then removed false-positives and noisy detections from within clusters by eliminating the largest 2% of roost sizes (>1.2 million birds), based on maximum roost sizes detected by manually screened roost data (Station KOKX, 1995-2023). Finally, to remove site-specific outliers, we applied a 2-dimensional kernel-density outlier detection estimation algorithm to each set of clustered points (Hyndman 1996, Węglarczyk 2018). We applied this algorithm to

each cluster's scatterplot of emergence date and log10-transformed bird count estimate, removing a percentage of outliers based on the total number of points within each cluster (i.e. 1% of outliers for 1000 detections, 10% outliers for 5 detections). The scale of outlier % to number of points was determined by manually screening a subset of clusters with varying sample sizes (See Supp. Fig. 3 for exemplary scatterplots). Finally, we calculated the mean centers of our filtered and clustered roost detections to reduce spatial range error from radar-determined roost sites (Kelly & Pletschet 2018), providing us with a filtered dataset of each roost's site ID, mean-center coordinates, and estimated daily size.

Estimating Roost Species Composition

Based on past observations of roost species compositions, we expected our initial dataset to contain roosts composed of other species, primarily Purple Martins (*Progne subis*), as well as relatively minute amounts of other swallow spp. (Burney 2002, Kelly et al. 2012). Fortunately, Purple Martins and Tree Swallows largely differ in their migratory timing and locations, with Purple Martins migrating slightly earlier and roosting more often in urban and forested habitats (Fink et al. 2023). We took advantage of these differences to eliminate Purple Martin roosts from our dataset. By cross-referencing radar-derived roost detections with weekly tree swallow and Purple Martin eBird abundance rasters (Fink et al. 2023), we created species abundance ratios for each roost site. To do this, we first collected weekly 27×27km rasters of both Tree Swallow and Purple Martin abundance rates, and assigned weekly values to daily roost detections. We then spatially joined raster values of both species to each roost for each week, and created simple species ratios using the abundance rates. We did not average/aggregate species abundance ratios across time, as the species composition of roosts can change within seasons in accordance to phenological mismatches between species (Burney 2002). By removing daily roost occurrences

that had <90% Tree Swallow abundance (40.7% of all valid roost detections) we were able to confidently remove migratory Purple Martin roosts from our analysis.

Network Construction

The primary goal in our network construction was to make a network that could effectively be processed by the Infomap Ecology R package to detect communities of roosts and their persistence across years (Rosvall & Bergstrom 2008, Rosvall et al. 2009). To accomplish this, we stacked annual roost networks together to create a directed multiplex network, and connected roost sites between years to maintain temporal cohesion of roost identities and roost community identities. Both spatial and temporal connections (edges) were assigned weights as indexes of connectivity. Thus, our network was made of roost-nodes with both weighted spatial and temporal edges (Fig. 1). Temporal edges were created to maintain roost identity and were formed only between sequential years of reoccurring roost sites, with weights being the average roost size in the latter year. The spatial edges were weighted by the estimated total number of birds that moved between co-occurring adjacent roosts each year.

Spatial directed edge weights were assigned as annual sums of daily estimated movements of birds from roost *i* to roost *j*, incorporating **a)** the following morning's roost size (*N*), **b)** the probability an individual switches roosts, and **c)** a distance-decay factor determined from the distances of sampled roost-to-roost movements. The full spatial-edge formula was:

$$w_{ij,t} = 0.22 \cdot N_{i,t} \cdot \frac{e^{-\beta d_{ij}}}{\sum_{k \in S(i)} e^{-\beta d_{ik}}} \quad (1)$$

where $w_{ij,t}$ is the expected number of birds switching from roost i to roost j on day t, 0.22 is the probability of roost switching (Laughlin et al. 2014), $N_{i,t}$ is the source roost size at day t, d is the distance (km) between roosts, $S(i)$ is the set of all neighboring roosts (≤60km; max 50km + 10km buffer) from roost i (to normalize the total movement across multiple adjacent roosts), and β is the distance-decay parameter (0.1017) derived from Laughlin et al. (2014)'s tracked individuals (Figure 1c).

Final directed spatial weights (W_{ij}) were then calculated as the sum of daily values across all days in the staging season, as shown in equation 2:

$$W_{ij} = \sum_{t=1}^{T} \cdot w_{ij,t} \quad (2)$$

Considering the roost-switching rate was derived from a small sample of individual movements (n = 15), we tested the values influence on our results by re-constructing our model with varying roost-switching values (0.1, 0.2, 0.3, and 0.4) and found no changes in weight distributions (Supp. Fig. 2). Thus, our weight calculations may be interpreted as an index of bird movement, but the use of .22 movement rates represent our closest estimation to the true number of birds moving between roosts each year.

Community Detection

With the multiplex network created, our final step before analysis was to delineate communities of roosts. To assign communities to our constructed network, we used the InfoMap algorithm (Rosvall et al. 2009), which is a random-walk algorithm that detects modules in networks. As random walks tend to move within "clusters" of nodes, the distribution of movements within and between modules can be used as a metric for community delineation. To do this, the InfoMap algorithm creates trial runs with different randomly assigned module partitions, and for each trial, the information content of a random walk's path (measured in bits) are compressed to

create a "codelength" value. The module assignment with the lowest resulting codelength (least movement between modules) represents the most accurate approximation of delineated roost communities.

The algorithm was applied with the R package "Infomapecology" (Edler et al. 2025), which used the directed edge weights as random walk movement probabilities. Two-level community detection was run with 50 random-walk trials, an unlimited upper relax rate, and no lower relax rate, allowing module identities to persist through years even if roosts were not consistently present.

Random-Network Testing

We constructed a multiplex network with empirically derived behavioral characteristics and roost-size estimates, which, without true movement data, represents only an approximation of the true movement network. To test if migratory Tree Swallows do form distinct roost communities, we compared our multiplex network structure to null model networks which were created with randomized edge strengths. By observing statistically significant differences in the characteristics of the constructed network and the randomized networks, we may eliminate the possibility of our constructed network being driven by random movements (Farine et al. 2017).

We tested nonrandom community structure with two complementary metrics measuring both community delineation and centralization. Community delineation was measured with the Infomapecology product "**codelength**", where lower values indicate high delineation of communities, and higher values indicate more diffuse communities (Smiljanić et al. 2023). Our second metric, community centralization, was measured with the **Gini coefficient** (Dorfman 1979). The Gini index is commonly used in macroeconomics to measure income inequality (Lopez et al. 2003, Kalmijn 2014), but is also used in assessing flow across networks (Hu and Wang 2005,

Lopes et al. 2012, Ma & Wang 2012, Kelly 2012). In this study, Gini coefficients were used to assess the distribution of bird movements between roosts within each community. We measured community-level Gini coefficients using each node's strength (cumulative incoming and outgoing spatial edge weights). Higher Gini values reflect greater inequality of movements between roosts, suggesting that central hub roosts dominate the flow of community-movement, while lower Gini values reflect a more even dispersion of movement potential among roosts.

To assess whether community structure was non-random, we compared our network's codelength and average Gini values to those from 100 "null" networks. These randomly generated null networks retain the same nodes and edges as our true network, yet the edge weights are shuffled within each year, creating a conservative null model which contains many of the original network's properties. If our true network's values fell outside the central 95% of the distribution of null-model values, they would be considered non-random, providing evidence that the observed networks structure reflects genuine ecological processes and justify meaningful interpretation.

Abundance Modelling

We aimed to first analyze how the network's overall size relates to population size. To do this, we inspected the network's scale, examining annual abundance-metrics of the network's functional components: total birds, total roosts and total communities. Our primary metric for network abundance was its **Total Number of Birds**, calculated as the annual sum of all roosts' mean daily bird counts. This metric refers solely to the population of birds in large and persistent roosts within the sampling range, and can only be interpreted as an index for the overall abundance of the network. We could not use ground-survey data for population trends as there is insufficient data to discern which breeding populations make up which roosts. We also assessed the total **Number of Roosts**, being the sum of all persistent roosts (≥10 detections) occurring within a given

year, and the **Number of Communities**, defined as the sum of all Infomap-derived communities containing at least three roosts. Determining the temporal trends of these descriptive characteristics provide baseline trends which can function as context when interpreting more systemic network characteristics.

The next step was to see how changes in network scale influence its community composition. In response to changing population sizes, does the composition of the networks units change proportionally? This involved assessing the networks **Mean Roost Size**, defined as the mean of each roost's annual average number of birds, **Mean Community Bird Count**, which represents the sum of each communities mean roost sizes, and **Mean Roost Count per Community**, being the average number of roosts within communities of ≥3 roosts. Understanding these metrics allows us to determine how the fundamental structural components of communities are impacted by population changes, and may further inform us of the network's topological dynamics.

The last major step was to understand how population sizes influence the underlying structure of the movement network. To achieve this, we assessed the distribution of bird movements between roosts within communities using the **Mean Community Gini Coefficient**, calculated with the "ineq" R package (Zeileis & Kleiber, 2014). Based on the distribution of node strengths, higher Gini values indicate that estimated roost-to-roost movement is concentrated through a small number of roosts, whereas lower values indicate more evenly distributed movement among roosts. To evaluate network connectivity, we calculated the **Mean Roost Degree** (the mean of every roost's total connections, excluding isolated roosts). To measure network density, we used the **Global Clustering Coefficient**, which is the ratio of triplets to the

total number of connected triplets within each subnetwork, normalized across all subnetworks. Global Clustering Coefficient was calculated with the igraph R package (Csárdi et al. 2026).

We modeled the temporal and abundance-dependent variation of these network characteristics using a combination of linear and generalized additive models (GAMs), the latter of which is notably useful for evaluating time series of nonlinear trends (Gleich et al. 2022, Heit et al. 2024). To evaluate the response of the characteristics to bird abundance, we aimed to first determine nonlinearity of structural trends, then determine whether the trend was a product of either bird abundance, time, or an interactive effect of both. We fit 6 models per response variable; a linear and additive fit to 1) year-only, 2) abundance-only, and 3) an interactive effect of year and abundance. All GAMs were fitted with thin plate regression splines using the "mgcv" package in R (Wood 2025) with maximum likelihood estimations.

Models were compared using Akaike Information Criterion (AIC) to evaluate relative support while accounting for model complexity, and well-fit models with the lowest AIC values were chosen for interpretation. Because AIC penalizes smoothness strongly at small sample sizes (n = 19 years), linear and nonlinear models frequently had $\Delta AIC < 2$, indicating comparable support (Supp. Tbl. 1). In these cases, we retained the GAMs for inference as they better captured nonlinear ecological processes such as fragmentation, centralization, and abundance-dependent restructuring.

Results

Network Description

Throughout all years of our final dataset, we found an annual average of 86.53 roosts (IQR 77-96.5) making up an average of 19.1 communities (IQR 16-23.5). Interestingly, the average number of days a roost persisted in a given year was 50.5, which is comparable to the finding of

Knight et al. (2018) of individual stopover stays lasting an average of 58 days. The median estimated number of birds in a roost was 10,709 but reached a maximum of 940,102 birds (IQR 4,238-27,646). These results should be interpreted with caution as radar-derived bird counts contain multiple sources of error which are primarily the inability to consistently capture all birds within a scan at once, sampling range error, and noise interference (mainly from weather and anomalous propagation).

Communities contained an average of 3 roosts (IQR 2-4), reaching up to 9 roosts. In a given year however, ~34% of detected roosts were isolates, while another ~20% were dyads (pairs of connected roosts). The top 5 longest-lived communities (occurring for >18 years) with the largest total bird counts were, from largest to smallest, in the Upper Delaware Bay, the Long Island Sound, the North Carolina Outer Coastal Basin, the Lower western Chesapeake Bay (estuaries between the James and the Rappahannock Rivers), and the southern coasts of Rhode Island and Massachusetts.

Null Modelling Results

To determine the validity of our constructed migratory network and identify biologically driven emergent properties, we compared metrics of our constructed "true" network to those of 100 randomized networks. We compared the network's codelengths to test for nonrandom modular structure, and average Gini coefficients to test for evenness of bird flow between roosts within communities. Our true network's codelength was 2.12, which was significantly lower than the codelengths of any of our random-generated networks (mean 2.354, IQR 2.32-2.39, Fig. 2). Our true network's average Gini Coefficient was 0.298, which was also lower than any of our randomly generated networks (mean 0.331, IQR .326-.335, Fig. 2). These results suggest that our constructed

network reflects emergent organization of communities in a decentralized movement network, with nonrandom distributions of movement within communities.

Network Scale

Our temporal modelling revealed significant relationships between either year and/or bird abundance for all metrics studied (Table 1). Throughout the sampling period, the constructed network exhibited a general trend of contraction (Fig. 3). The trend in total abundance of all detected roosting birds was best captured by a GAM with year alone ($p < 0.01$). Network abundance declined from ~3.75 million birds in 2005 to ~2.5 million in 2016, before partially recovering to ~3 million in 2023 (Fig. 4a). Despite the partial recovery in bird abundance, the scalar components of the network experienced a continuous decline over time, with the total number of roosts declining by -22% and the number of communities by -50% (Fig. 4b, c). Both of these metrics were best explained by interactive GAMs which included year and bird abundance ($p < 0.01$).

Network Composition

As the scale of the network declined, the network's composition displayed significant changes. The average size of roosts had a similar trend to that of the overall bird abundance, declining dramatically from 2005-2016 (-46%), then recovering near initial levels (~250k birds/roost) by 2023 (Fig. 4d). Interestingly, the average size of communities remained relatively stable as total abundance declined, until 2018, when it began to increase from ~125k birds to ~190k birds by 2023 (Fig. 4e). The average number of roosts per community grew steadily from ~4.5 roosts per community in 2005 to ~6 in 2023 (Fig. 4f). All three metrics were best explained by interactive GAMs of year and bird abundance ($p < 0.01$).

Network Topology

As birds consolidated into larger communities, the network's topology exhibited an overall decrease in connectivity, while movement within communities became more centralized. The average Gini coefficient of communities, representing the distribution of movement within communities, increased by 32% across the sample period, indicating greater heterogeneity of bird concentration within communities (Fig. 4g). This trend was best described by a GAM of total bird abundance alone ($p < 0.05$).

Despite communities growing in the number of birds and roosts, the average roost degree (number of roost neighbors) declined from ~2 in 2005 to ~1.5 in 2023, and was best modeled as a univariate GAM response to year alone. This trend in connectivity was also reflected in the annual global clustering coefficient, which declined by 14%, being best explained by a linear effect of bird abundance alone ($p < 0.05$).

Discussion

This study is the first of its kind to analyze a single-species movement network on a continental and multi-decadal scale. Through studying the temporal dynamics of this movement network's structure, we found strong evidence that such "aggregations of aggregations" can sustain cohesive structures across continents and over decades and can adapt in complex ways when faced with demographic changes.

Our null model comparisons strongly suggest that the constructed network reflects biologically driven processes and validates the novel methods as sound for analyzing roost networks on a continental scales. The null model comparisons also revealed inherent modularity in migratory Tree Swallow roosts, uncovering a formerly unknown characteristic of roosting

behavior while setting the stage for future work to determine the drivers behind roost clustering and roost switching.

Over the course of 19 years, the network's structure exhibited a complex and intertwined relationship with its abundance, exhibiting shifts in scale, composition, and topology as the population declined between 2005 and 2015 (Fig. 4). At the beginning of the study period, the network was at its largest, exhibiting the highest abundance of birds (~3.75 million) and roost sites (~150). Communities were composed of relatively few roosts (~4.5) and birds, but were abundant across the landscape. Movements within these communities were relatively evenly distributed (as determined by their Gini coefficients) and roosts were at their highest levels of local and global connectivity. However, the subsequent decades revealed declines in overall bird abundance, and evidence of a structural shift in the network that persisted even after bird abundance stabilized at its lowest size.

Following the population's stabilization at its lowest abundance, the composition of its nodes and communities began to restructure themselves. Following the stabilization in ~2015, roost sizes recovered moderately (~250,000 birds) and the sizes of communities surged beyond their consistent low levels held throughout the first decade, likely caused by smaller roosts being more likely to dissolve, leaving predominantly large persistent roosts (Fig. 4d, 4e). To maintain preferred community densities within a shrinking landscape, the system likely consolidated its roosts around persistent coastal communities, as the average number of roosts per community increased from ~4.5 to ~6. This consolidation suggests a survival strategy where birds aggregate at the most persistent sites, trading spatial ubiquity for the potential social information-sharing and anti-predator benefits provided by the larger communities.

As these remaining communities became more concentrated, they also exhibited changes in how birds moved within them, leading to increased community centralization (rising Gini coefficients) and decreased global clustering, signaling a transition from a decentralized and broad network to a less connected and narrower network with more centralized communities.

Our results suggest that once a certain abundance of birds was no longer sustained, the network entered a state of structural inertia where the stabilization of the population at a lower overall abundance did not necessitate a proportional stabilization of the network's structure. This reflects common characteristics found among complex systems, where their structural resilience can depend on a certain abundance of components. Overall, this study indicates that Tree Swallow roosts, and their regular exchanging of individuals, can be understood as a dynamic and adaptive complex system that is experiencing significant contraction and fragmentation.

Implications

Our temporal and population modelling suggests that migratory Tree Swallow roost networks respond to population declines by contracting their network into fewer communities with more (albeit smaller) roosts, and more decentralized roost-to-roost movements. The nonlinear patterns also reflect characteristics similar to networks based on information-exchange, though this cannot be confirmed to be the case for swallow roosts without direct observation.

In the highly connected network of 2005, bird movement was distributed across many alternative pathways, providing a high degree of connectivity and potential resilience. If a single roost were lost, the surrounding network could easily absorb the flow. In the 2023 state, however, connections between roosts were less frequent, particularly in the inland range, and movement was increasingly funneled through a shrinking number of critical "hub" roosts. This centralization of communities has likely created systemic bottlenecks where the integrity of the migratory corridor

now rests on a smaller number of high-traffic nodes. Consequently, the network has become topologically brittle: the localized loss of a single hub today would likely have a disproportionately negative impact on the network's flow.

This study highlights not only the critical conservation needs of remaining occupied roost sites, but also how roost sites can be prioritized based on their historical role in their roost communities. Additionally, existing isolated roosts are also crucial for protection, as they can likely facilitate the reconstruction of communities upon population growth.

Beyond site-level conservation, these findings suggest that aggregation network structure may function as a sensitive indicator of population health more broadly. A passive monitoring effort of aggregation network structure via weather radar could provide a system-level population health metric that is spatially comprehensive and independent of ground-based survey effort.

Limitations

Certain limitations in our methods should be noted, starting with radar-derived roost-size estimations, which have a moderate range of error due to distance-sampling (Kelly 2012). Despite this limitation, the scale of our dataset and consistency in annual metrics indicate largely accurate delineation of roost communities and comparable size estimates. Another limitation lies in our exclusion of ephemeral roosts in the constructed network, which creates a data gap in our bird abundance metric. However, visual comparison of Breeding Bird Survey data of Tree Swallow population trends in the North Atlantic Forest seem to have a similar trend to that of our radar-derived abundance. This is not a validation of our abundance metric, nor negates the limitation of excluding ephemeral roosts, but is suggestive that large-scale weather radar networks may be capable of estimating bird population trends (Ziolkowski et al. 2023). Lastly, our movement rules were derived from limited roost-to-roost movement data (n = 15 tracked individuals) during the

nonbreeding season, which may have different patterns from our studied migratory roosts and would not capture potential spatiotemporal relationships in roost-switching behaviors.

Recommendations

Further work should determine the individual-level motivations of roost switching and better understand the impact of roost connectivity on fitness and survival. Future roost networks developed with radar-derived data have a plethora of avenues to explore, such as testing connectivity in relation to habitat associations and/or phenological trends, evaluating factors that influence roost and community persistence, comparing structural characteristics between migratory and nonbreeding communities, assessing network degree distributions, or determining connectivity between breeding populations and roost communities, all of which are likely fruitful endeavors in uncovering the dynamics of aerial insectivore roosts and the complexity of animal aggregations.

References

August, T.A., M.A. Nunn, A.G. Fensome, D.M. Linton, and F. Mathews. (2014) Sympatric woodland Myotis bats form tight-knit social groups with exclusive roost home ranges. PLOS ONE 9 (10), e112225. https://doi.org/10.1371/journal.pone.0112225.

Bascompte, J. (2007) Networks in ecology. Basic and Applied Ecology 8 (6), 485–490. https://doi.org/10.1016/j.baae.2007.06.003.

Beck, K.B., C.E. Regan, K. McMahon, et al. (2024) Experimental manipulation of population density in a wild bird alters social structure but not patch discovery rate. Animal Behaviour 209, 95–120. https://doi.org/10.1016/j.anbehav.2023.12.010.

Belotti, M.C.T.D., Y. Deng, W. Zhao, et al. (2023) Long-term analysis of persistence and size of swallow and Martin roosts in the US Great Lakes. Remote Sensing in Ecology and Conservation 9 (4), 469–482. https://doi.org/10.1002/rse2.323.

Bent, A.C. (1942) Life histories of North American flycatchers, larks, swallows, and their allies. Order Passeriformes (Families Cotingidae, Tyrannidae, Alaudidae, and Hirundinidae). http://hdl.handle.net/10088/10013.

Bridge, E.S., S.M. Pletschet, T. Fagin, et al. (2016) Persistence and habitat associations of Purple Martin roosts quantified via weather surveillance radar. Landscape Ecology 31 (1), 43–53. https://doi.org/10.1007/s10980-015-0279-0.

Burney, C.W. (2002) A study of swallow roosts found in the eastern United States. M.Sc. thesis, Cornell University.

Caccamise, D.F., and D.W. Morrison. (1986) Avian communal roosting: implications of diurnal activity centers. The American Naturalist 128 (2), 191–198. https://doi.org/10.1086/284553.

Chaverri, G. (2010) Comparative social network analysis in a leaf-roosting bat. Behavioral Ecology and Sociobiology 64 (10), 1619–1630. https://doi.org/10.1007/s00265-010-0975-3.

Cheng, Z., S. Gabriel, P. Bhambhani, et al. (2020) Detecting and tracking communal bird roosts in weather radar data. Proceedings of the AAAI Conference on Artificial Intelligence 34 (01), 378–385. https://doi.org/10.1609/aaai.v34i01.5373.

Chilson, C., K. Avery, A. McGovern, E. Bridge, D. Sheldon, and J. Kelly. (2019) Automated detection of bird roosts using NEXRAD radar data and convolutional neural networks. Remote Sensing in Ecology and Conservation 5 (1), 20–32. https://doi.org/10.1002/rse2.92.

Chilson, P.B., W.F. Frick, P.M. Stepanian, J.R. Shipley, T.H. Kunz, and J.F. Kelly. (2012) Estimating animal densities in the aerosphere using weather radar: to Z or not to Z? Ecosphere 3 (8), art72. https://doi.org/10.1890/ES12-00027.1.

Clements, C.F., M.A. McCarthy, and J.L. Blanchard. (2019) Early warning signals of recovery in complex systems. Nature Communications 10 (1), 1681. https://doi.org/10.1038/s41467-019-09684-y.

Csárdi, G., T. Nepusz, V. Traag, et al. (2026) igraph: network analysis and visualization. V. 2.3.0. https://cran.r-project.org/web/packages/igraph/index.html.

DeMott, W.G., A.N. Stillman, J.B. Kolb, and C.S. Elphick. (2023) NEXRAD highlights the effects of wind and date at a Tree Swallow (Tachycineta bicolor) roost during fall migration. The Wilson Journal of Ornithology 134 (4), 623–632. https://doi.org/10.1676/21-00084.

Deng, Y., M.C.T.D. Belotti, W. Zhao, et al. (2023) Quantifying long-term phenological patterns of aerial insectivores roosting in the Great Lakes region using weather surveillance radar. Global Change Biology 29 (5), 1407–1419. https://doi.org/10.1111/gcb.16509.

Dorfman, R. (1979) A formula for the Gini coefficient. The Review of Economics and Statistics 61 (1), 146–149. https://doi.org/10.2307/1924845.

Drake, J.M., and B.D. Griffen. (2010) Early warning signals of extinction in deteriorating environments. Nature 467 (7314), 456–459. https://doi.org/10.1038/nature09389.

Dunne, J.A., R.J. Williams, and N.D. Martinez. (2002) Network structure and biodiversity loss in food webs: robustness increases with connectance. Ecology Letters 5 (4), 558–567. https://doi.org/10.1046/j.1461-0248.2002.00354.x.

Dunning, J.B., Jr. (2007) CRC handbook of avian body masses. CRC Press.

Eastwood, E., G.A. Isted, and G.C. Rider. (1962) Radar ring angels and the roosting behaviour of starlings. Proceedings of the Royal Society of London. Series B. Biological Sciences 156 (963), 242–267. https://doi.org/10.1098/rspb.1962.0042.

Edler, D., A. Holmgren, and M. Rosvall. (2025) The MapEquation software package. https://mapequation.org.

Esri. (2024) Density-based clustering (Spatial Statistics). ArcGIS Pro documentation, Version 3.4. https://pro.arcgis.com/en/pro-app/latest/tool-reference/spatial-statistics/densitybasedclustering.htm.

Ester, M., H.P. Kriegel, J. Sander, and X. Xu. (1996) A density-based algorithm for discovering clusters in large spatial databases with noise. Proceedings of the 2nd International Conference on Knowledge Discovery and Data Mining, 226–331. https://ui.adsabs.harvard.edu/abs/1996kddm.conf..226E.

Evangelista, D.J., D.D. Ray, S.K. Raja, and T.L. Hedrick. (2017) Three-dimensional trajectories and network analyses of group behaviour within Chimney Swift flocks during approaches to the roost. Proceedings of the Royal Society B: Biological Sciences 284 (1849), 20162602. https://doi.org/10.1098/rspb.2016.2602.

Farine, D.R. (2017) A guide to null models for animal social network analysis. Methods in Ecology and Evolution 8 (10), 1309–1320. https://doi.org/10.1111/2041-210X.12772.

Fink, D., T. Auer, A. Johnston, M. Strimas-Mackey, S. Ligocki, O. Robinson, W. Hochachka, L. Jaromczyk, C. Crowley, K. Dunham, A. Stillman, I. Davies, A. Rodewald, V. Ruiz-Gutierrez, and C. Wood. (2023) eBird status and trends, data version: 2022. Cornell Lab of Ornithology, Ithaca, New York. https://doi.org/10.2173/ebirdst.2022.

Fortuna, M.A., A.G. Popa-Lisseanu, C. Ibáñez, and J. Bascompte. (2009) The roosting spatial network of a bird-predator bat. Ecology 90 (4), 934–944. https://doi.org/10.1890/08-0174.1.

Gleich, S.J., J.A. Cram, J.L. Weissman, and D.A. Caron. (2022) NetGAM: using generalized additive models to improve the predictive power of ecological network analyses constructed using time-series data. ISME Communications 2 (1), 23. https://doi.org/10.1038/s43705-022-00106-7.

Hassanien, A.E., and E. Emary. (2018) Swarm intelligence: principles, advances, and applications. CRC Press.

Heit, D.R., W. Ortiz-Calo, M.K.P. Poisson, A.R. Butler, and R.J. Moll. (2024) Generalized nonlinearity in animal ecology: research, review, and recommendations. Ecology and Evolution 14 (7), e11387. https://doi.org/10.1002/ece3.11387.

Horton, K.G., B.M. Van Doren, F.A. La Sorte, E.B. Cohen, H.L. Clipp, J.J. Buler, D. Fink, J.F. Kelly, and A. Farnsworth. (2019) Holding steady: little change in intensity or timing of bird migration over the Gulf of Mexico. Global Change Biology 25 (3), 1106–1118. https://doi.org/10.1111/gcb.14540.

Hostetler, J.A., J.R. Sauer, J.E. Hines, D. Ziolkowski, and M. Lutmerding. (2024) The North American Breeding Bird Survey, analysis results 1966–2023. U.S. Geological Survey. https://doi.org/10.5066/P1F2X4WH.

Hu, H.B., and L. Wang. (2005) The Gini coefficient's application to general complex networks. Advances in Complex Systems 08 (01), 159–167. https://doi.org/10.1142/S0219525905000385.

Hughey, L.F., A.M. Hein, A. Strandburg-Peshkin, and F.H. Jensen. (2018) Challenges and solutions for studying collective animal behaviour in the wild. Philosophical Transactions of the Royal Society B: Biological Sciences 373 (1746), 20170005. https://doi.org/10.1098/rstb.2017.0005.

Hyndman, R.J. (1996) Computing and graphing highest density regions. The American Statistician 50 (2), 120–126. https://doi.org/10.1080/00031305.1996.10474359.

Kalmijn, W. (2014) Gini coefficient. In Encyclopedia of Quality of Life and Well-Being Research. Springer, Dordrecht. https://doi.org/10.1007/978-94-007-0753-5_1168.

Kelly, G. (2012) Gini coefficients, social network analysis, and Markov chains: quantitative methods for analyzing the distribution of benefits in natural resource-dependent communities. M.Sc. thesis, Simon Fraser University. https://summit.sfu.ca/item/12403.

Kelly, J.F., J.R. Shipley, P.B. Chilson, K.W. Howard, W.F. Frick, and T.H. Kunz. (2012) Quantifying animal phenology in the aerosphere at a continental scale using NEXRAD weather radars. Ecosphere 3 (2), art16. https://doi.org/10.1890/ES11-00257.1.

Kelly, J.F., and S.M. Pletschet. (2018) Accuracy of swallow roost locations assigned using weather surveillance radar. Remote Sensing in Ecology and Conservation 4 (2), 166–172. https://doi.org/10.1002/rse2.66.

Knight, S.M., D.W. Bradley, R.G. Clark, et al. (2018) Constructing and evaluating a continent-wide migratory songbird network across the annual cycle. Ecological Monographs 88 (3), 445–460. https://doi.org/10.1002/ecm.1298.

Laughlin, A.J., D.R. Sheldon, D.W. Winkler, and C.M. Taylor. (2014) Behavioral drivers of communal roosting in a songbird: a combined theoretical and empirical approach. Behavioral Ecology 25 (4), 734–743. https://doi.org/10.1093/beheco/aru044.

le Roux, C.E., and J.J. Nocera. (2021) Roost sites of Chimney Swift (Chaetura pelagica) form large-scale spatial networks. Ecology and Evolution 11 (9), 3820–3829. https://doi.org/10.1002/ece3.7235.

Lewis, S.E. (1995) Roost fidelity of bats: a review. Journal of Mammalogy 76 (2), 481–496. https://doi.org/10.2307/1382357.

Lopes, G.R., R. da Silva, M.M. Moro, and J.P.M. de Oliveira. (2012) Scientific collaboration in research networks: a quantification method by using Gini coefficient. International Journal of Computer Science and Applications 9 (2), 15–31.

López, H. (2003) Macroeconomics and inequality. The World Bank, Washington, DC.

Ma, C., and X. Wang. (2012) Application of the Gini correlation coefficient to infer regulatory relationships in transcriptome analysis. Plant Physiology 160 (1), 192–203. https://doi.org/10.1104/pp.112.201962.

MacGregor, H.E.A., J.E. Herbert-Read, and C.C. Ioannou. (2020) Information can explain the dynamics of group order in animal collective behaviour. Nature Communications 11 (1), 2737. https://doi.org/10.1038/s41467-020-16578-x.

Murray, B.G., Jr. (1969) Ecological adaptations for breeding in birds. The Auk 86 (4), 774–777. https://doi.org/10.2307/4083484.

Parrish, J.K., and L. Edelstein-Keshet. (1999) Complexity, pattern, and evolutionary trade-offs in animal aggregation. Science 284 (5411), 99–101. https://doi.org/10.1126/science.284.5411.99.

Perez, G., W. Zhao, Z. Cheng, M.C.T.D. Belotti, Y. Deng, V.F. Simons, E. Tielens, J.F. Kelly, K.G. Horton, S. Maji, and D. Sheldon. (2024) Using spatiotemporal information in weather radar data to detect and track communal roosts. Remote Sensing in Ecology and Conservation 10 (5), 567–583. https://doi.org/10.1002/rse2.388.

Rhodes, M., G.W. Wardell-Johnson, M.P. Rhodes, and B. Raymond. (2006) Applying network analysis to the conservation of habitat trees in urban environments: a case study from Brisbane, Australia. Conservation Biology 20 (3), 861–870. https://doi.org/10.1111/j.1523-1739.2006.00415.x.

Rosvall, M., and C.T. Bergstrom. (2008) Maps of random walks on complex networks reveal community structure. Proceedings of the National Academy of Sciences 105 (4), 1118–1123. https://doi.org/10.1073/pnas.0706851105.

Rosvall, M., D. Axelsson, and C.T. Bergstrom. (2009) The map equation. The European Physical Journal Special Topics 178 (1), 13–23. https://doi.org/10.1140/epjst/e2010-01179-1.

Russell, K.R., and S.A. Gauthreaux. (1998) Use of weather radar to characterize movements of roosting Purple Martins. Wildlife Society Bulletin 26 (1), 5–16.

Smiljanić, J., C. Blöcker, A. Holmgren, D. Edler, M. Neuman, and M. Rosvall. (2023) Community detection with the map equation and Infomap: theory and applications. arXiv:2311.04036. https://doi.org/10.48550/arXiv.2311.04036.

Spiller, K.J., and R. Dettmers. (2019) Evidence for multiple drivers of aerial insectivore declines in North America. The Condor: Ornithological Applications 121 (2), duz010. https://doi.org/10.1093/condor/duz010.

Stützle, T., M. López-Ibáñez, and M. Dorigo. (2011) A concise overview of applications of ant colony optimization. Wiley Encyclopedia of Operations Research and Management Science. John Wiley & Sons, Ltd. https://doi.org/10.1002/9780470400531.eorms0001.

Sumpter, D.J.T. (2006) The principles of collective animal behaviour. Philosophical Transactions of the Royal Society B: Biological Sciences 361 (1465), 5–22. https://doi.org/10.1098/rstb.2005.1733.

Tang, J., G. Liu, and Q. Pan. (2021) A review on representative swarm intelligence algorithms for solving optimization problems: applications and trends. IEEE/CAA Journal of Automatica Sinica 8 (10), 1627–1643. https://doi.org/10.1109/JAS.2021.1004129.

Trøjelsgaard, K., and J.M. Olesen. (2016) Ecological networks in motion: micro- and macroscopic variability across scales. Functional Ecology 30 (12), 1926–1935. https://doi.org/10.1111/1365-2435.12710.

Van Den Broeke, M.S. (2019) Radar quantification, temporal analysis and influence of atmospheric conditions on a roost of American Robins (Turdus migratorius) in Oklahoma. Remote Sensing in Ecology and Conservation 5 (2), 193–204. https://doi.org/10.1002/rse2.99.

Ward, P., and A. Zahavi. (1973) The importance of certain assemblages of birds as 'information-centres' for food-finding. Ibis 115 (4), 517–534. https://doi.org/10.1111/j.1474-919X.1973.tb01990.x.

Watts, B.D., and R.J. Dyer. (2018) Structure and resilience of Bald Eagle roost networks. Wildlife Society Bulletin 42 (2), 195–203. https://doi.org/10.1002/wsb.865.

Węglarczyk, S. (2018) Kernel density estimation and its application. ITM Web of Conferences 23, 00037. https://doi.org/10.1051/itmconf/20182300037.

Winkler, D.W. (2006) Roosts and migrations of swallows. Hornero 21 (2), 85–97.

Wood, S. (2025) mgcv: mixed GAM computation vehicle with automatic smoothness estimation. V. 1.9-3. https://cran.r-project.org/web/packages/mgcv/index.html.

Zeileis, A., and C. Kleiber. (2014) ineq: measuring inequality, concentration, and poverty. V. 0.2-13. https://cran.r-project.org/web/packages/ineq/index.html.

Zeus, V.M., C. Reusch, and G. Kerth. (2018) Long-term roosting data reveal a unimodular social network in large fission-fusion society of the colony-living Natterer's bat (Myotis nattereri). Behavioral Ecology and Sociobiology 72 (6), 99. https://doi.org/10.1007/s00265-018-2516-4.

Ziolkowski, D.J., M. Lutmerding, W.B. English, V.I. Aponte, and M.A.R. Hudson. (2023) North American Breeding Bird Survey dataset 1966–2022. U.S. Geological Survey data release. https://doi.org/10.5066/P9GS9K64.

Table 1. Top Model Results

Response Variable	Model Structure	edf	F	p-value	Adj. R^2	Dev. Expl.
Total Bird Count	`s(year)`	2.897	11.83	0.000216	0.699	74.8%
Total Number of Roosts	`te(year, n_birds)`	4.099	11.85	0.000148	0.749	80.6%
Number of Communities	`te(year, n_birds)`	3.339	29.35	3.1×10^{-6}	0.825	85.4%
Average Roost Size	`te(year, n_birds)`	4.325	31.08	$< 2 \times 10^{-16}$	0.895	92.0%
Mean Community Size	`te(year, n_birds)`	5.339	6.408	0.00706	0.575	65.4%
Avg Roosts per Community	`te(year, n_birds)`	9.846	7.291	0.00205	0.781	90.1%
Mean Gini Coefficient	`s(n_birds)`	1.000	7.23	0.0155	0.257	29.8%
Mean Roost Degree	`s(year)`	4.295	10.38	0.000231	0.747	80.8%
Global Clustering Coefficient	`lm(n_birds)`†	—	8.317	0.0103	0.289	32.9%

Table 1: All GAMs fitted with thin plate regression splines using the R package "mgcv" (Wood 2025) with maximum likelihood estimation. Model selection based on AIC (Supp. Table 1); where $\Delta AIC < 2$ between linear and nonlinear fits, the GAM was retained to capture nonlinear ecological dynamics. Effective degrees of freedom (edf) reported for smooth terms; dashes indicate linear models with no smooth. F-statistics and p-values correspond to smooth terms (GAMs) or overall model F-test (linear models).

† Linear model selected over GAM te(year, n_birds) (edf = 16.6 on n = 19; overfit). Top defensible model: lm(clustering_coeff ~ n_birds). Adj. R^2 and Dev. Expl. reflect the linear model.

Figure 1. Outline of Network Properties

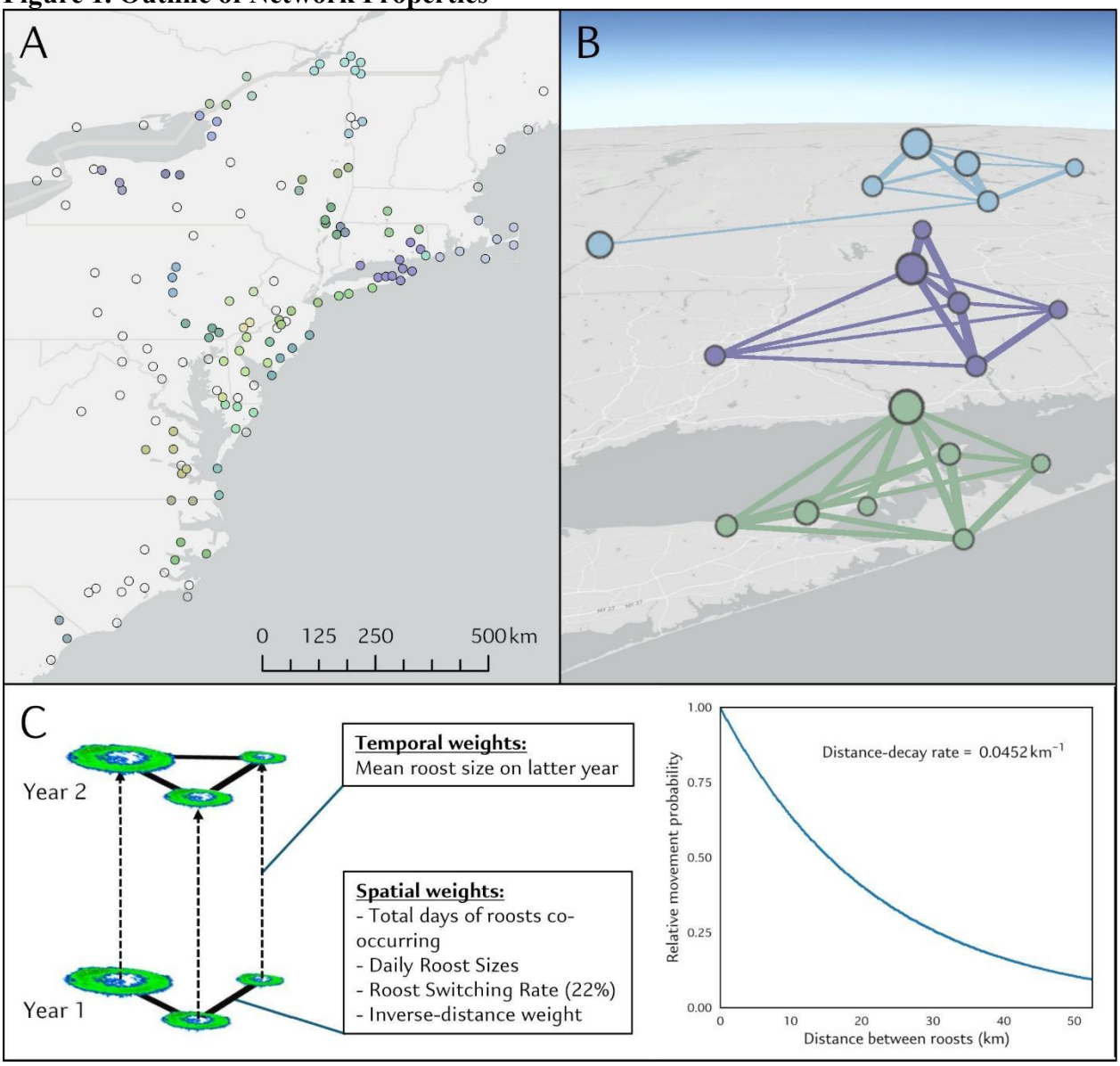


Figure 1. An exemplary outline of the roost-to-roost network construction. Panel A is a map representing each roost site used in constructing the network, colored by mode community membership across all years (transparent roosts are isolated). Panel B is a 3-D temporal visualization of the multiplex structure of the Long Island roost community over three years (layered from earliest to latest; 2005, 2015, 2023). Node sizes are determined by annual average roost size, edge widths are determined by distance between roosts (farther distances symbolized by thinner lines), and colors distinguish years. Panel C describes the factors used to calculate both temporal and spatial weights, in addition to a plot of the distance-decay distribution used to calculate inverse-distance weights. For the full formula used to calculate spatial weights, see formula 1.

Figure 2. Random-Network Metrics

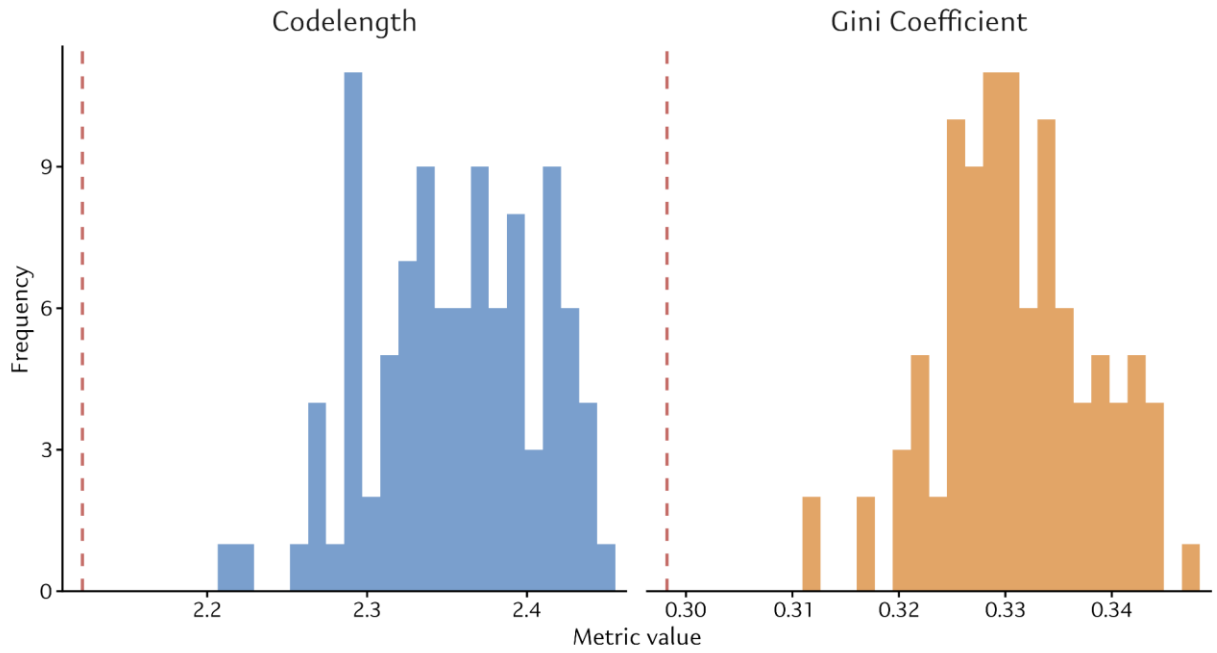


Figure 2. Histograms of randomized network characteristic values, with constructed network value indicated by the dashed red line. Both constructed network characteristics were outside of the 2.5-97.5% distribution of random-network characteristics, indicating non-random community-based structure in the constructed Tree Swallow Network.

Figure 3. Network Map 2005 and 2023

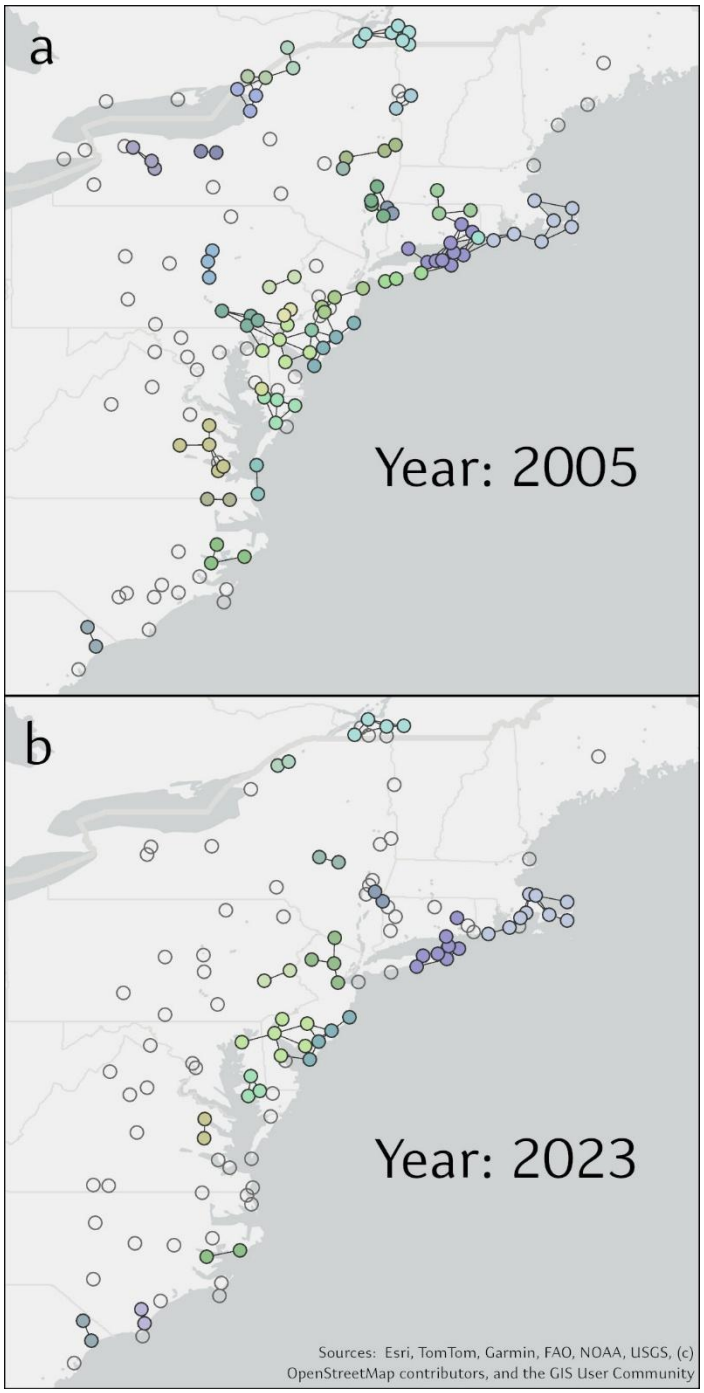


Figure 3. A faceted map showing change in network structure from 2005-2023. Community membership of roosts (nodes) are discerned by node color. Lines between nodes represent constructed roost-to-roost movements. Isolated roosts are represented as transparent circles.

Figure 4. Network Metric Time Series

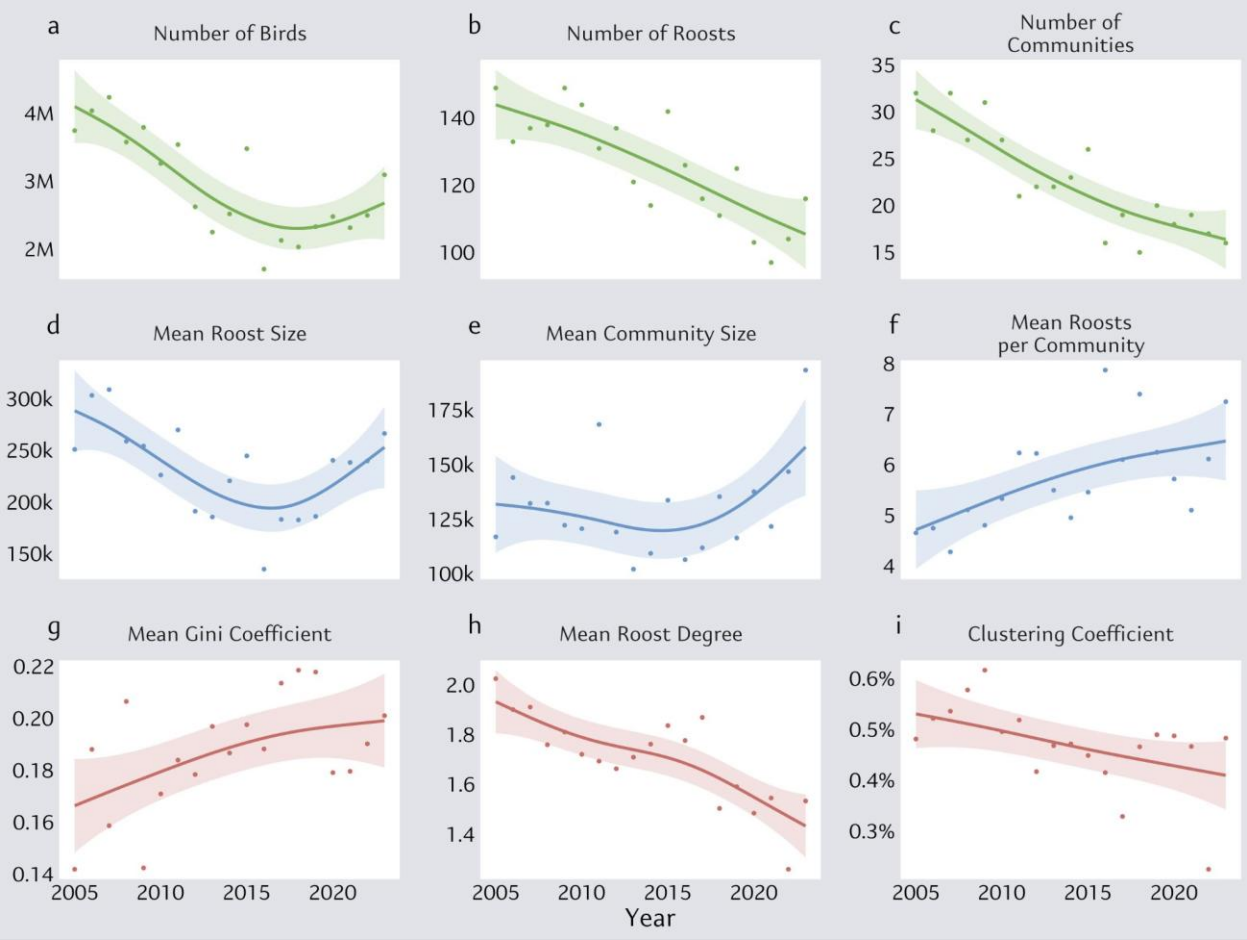


Figure 4. GAM-predicted trend-lines of population trend (number of birds) and respective network characteristics across years. Each line is a univariate general additive model prediction line shown for visualization purposes; top models for each variable are reported in Table 1. Plots are color-coded by metric categories (green is scale, dark blue is composition, and red is topology).

Supplementary Files

This is a list of supplementary files associated with this preprint. Click to download.

- SupplementaryMaterial.docx